

# Vulcanization Behavior and Mechanical Properties of Organoclay Fluoroelastomer Nanocomposites

Sriram Lakshminarayanan, Genaro A. Gelves, Uttandaraman Sundararaj

Department of Chemical and Petroleum Engineering, Schulich School of Engineering, University of Calgary, Calgary, Alberta, Canada T2N 1N4

Received 13 July 2011; accepted 13 September 2011

DOI 10.1002/app.35624

Published online 11 December 2011 in Wiley Online Library (wileyonlinelibrary.com).

**ABSTRACT:** The vulcanization behavior and mechanical properties of clay/fluoroelastomer nanocomposites produced by melt-mixing of Dyneon FPO 3741 (a terpolymer of vinylidene fluoride, hexafluoropropylene, and tetrafluoroethylene) with 10 phr of unmodified montmorillonite (CloisiteNA) or di(hydrogenated tallow-alkyl) dimethyl ammonium-modified montmorillonites (Cloisite15A and Cloisite20A) were studied. The properties of clay/FKM nanocomposites were compared with composites prepared using 10 and 30 phr of carbon black. The effects of clay surfactant and surfactant concentration on the vulcanization behavior, mechanical, and dynamical properties of peroxide cured composites were studied. XRD results of cured composites showed a decrease in d-spacing and indicated deintercalation of the clays after the vulcanization process. It was also found that organoclays retard the

FKM peroxide vulcanization process. Significantly, higher maximum torque on vulcanization was obtained with organoclays versus unmodified clay and carbon black. Although the morphologies of organoclay/FKM nanocomposites studied by XRD and TEM suggest similar intercalated/exfoliated structures, the organoclay with the lowest concentration of surfactant (95 meq/100 g clay) resulted in the highest increase in torque, modulus, hardness, and tear strength in the clay/FKM nanocomposites. It was also found that organoclays can increase both the hydrodynamic reinforcement and hysteresis loss of FKM nanocomposites. © 2011 Wiley Periodicals, Inc. *J Appl Polym Sci* 124: 5056–5063, 2012

**Key words:** fluoroelastomer; nanoclay; nanocomposites; mechanical properties; vulcanized rubber

## INTRODUCTION

Fluorocarbon rubber (FKM) is a specialty elastomer often used in severe and demanding environments. The main drawback of FKM stems from its low strength, which may limit its usage in many new areas. Carbon black has been the leading reinforcing filler for elastomers for many decades, primarily due to its ability to significantly improve mechanical properties and to reduce compound cost. However, an increased recent attention toward nanoclays arises from their ability to improve composite properties at a much lower loading when compared with conventional fillers like carbon black. Nanoclays have been proved to impart substantial mechanical strength to many thermoplastic polymer matrices at very low loadings when compared with conventional fillers.<sup>1,2</sup> Although thermoplastics and thermoset elastomers fall under the broad category of polymers, elastomers differ from thermoplastics in numerous methods. The foremost difference between elastomers and thermoplastics is vulcaniza-

tion of the elastomer matrix using curing agents. Therefore, in addition to applying the currently available technology on nanoclays, elastomer-specific parameters and processes need to be investigated.

There have been previous reports on the effect of nanoclay on vulcanization behavior of elastomer matrices.<sup>3–7</sup> There has been only one such study on FKM composites.<sup>8</sup> That work reported that the curing of FKM using diamines was accelerated by the presence of organically modified clays. In addition, changes in the morphology of clay/elastomer nanocomposites during the vulcanization process have been reported.<sup>9–11</sup> For instance, it has been found that high vulcanization pressure produced re-aggregation of individually dispersed clays, which may reduce the reinforcement effect of nanoclays on the composite.<sup>9</sup> This phenomenon has been observed for elastomers cured using diamine system. Fluoroelastomers can be also cross-linked using peroxide. However, the effect of nanoclays on peroxide curing behavior of FKM has not been formerly studied. Herein, the authors have selected a peroxide curing system due to the enhancement in thermal stability of the composites versus those cured with diamines.

In this study, the authors have studied the effect of unmodified clay and organoclays on the behavior of peroxide vulcanization of FKM and the mechanical properties of clay/FKM nanocomposites produced by

Correspondence to: U. Sundararaj (u.sundararaj@ucalgary.ca).

TABLE I  
Formulation of FKM Composites Used in this Study

Composites → materials↓	FKM	10CB	30CB	10NA	1015A	1020A
Filler	None	C-black N990	C-black N990	Clay CloisiteNA	Clay Cloisite15A	Clay Cloisite20A
Filler conc. (phr)	0	10	30	10	10	10
ZnO (phr)	3	3	3	3	3	3
TAIC (phr)	3	3	3	3	3	3
Peroxide (phr)	3	3	3	3	3	3

melt compounding. In our previous study, the authors have used melt compounding to study the effect of the surfactant type and the clay concentration on the rheological behavior and the morphology of unvulcanized clay/FKM nanocomposites.<sup>12</sup> The authors concluded that Cloisite<sup>®</sup> nanoclays 15A and 20A exhibit better compatibility with FKM matrix. Thus, a higher enhancement in mechanical properties of clay/FKM nanocomposites could be expected using these organoclays. Herein, the vulcanization, mechanical, and dynamic mechanical properties of organoclay/FKM nanocomposites are presented.

## EXPERIMENTAL

### Materials

Dyneon<sup>™</sup> FPO 3741, a terpolymer of vinylidene fluoride (VDF), hexafluoropropylene, and tetrafluoroethylene with fluorine content of 69.5%, specific gravity 1.89, and Mooney viscosity 38 ML (1 + 10) at 121°C was obtained from Dyneon, 3M. Nanoclays Cloisite<sup>®</sup> NA (untreated), 15A and 20A were obtained from Southern Clay Products. Medium thermal carbon black (Thermax N-990; Bulk density: 1.7–1.9 g/mL), peroxide curative (Triganox 101-45B-pc; 2,5-dimethyl-2,5-di-*t*-butylperoxyhexane), co-agent TAIC (SR533; triallylisocyanurate), and acid acceptor (ZnO) were donated by Cancarb, Akzo Nobel Polymer Chemicals, Sartomer, and L.V. Lomas.

### Nanocomposites preparation

Uncured FKM/Clay composites were prepared using the procedure described earlier.<sup>12</sup> The composites were further compounded with curing ingredients as follows: uncured FKM/clay composites were loaded in a Haake Rheomix Series 600 with Banbury blades. Then, ZnO (3 phr), TAIC (3 phr), and peroxide (3 phr) were added simultaneously and mixing was continued for 15 min. The temperature during mixing was maintained between 50 and 75°C to avoid scorching. Fill factor was 0.70 and rotation speed was 40 rpm. After mixing, the compound was removed from the mixer, cooled, and

pulled out as a sheet from a two-roll mill. The carbon black sample (10CB) was mixed at the same conditions. The rubber was initially masticated for 2 min and then the other ingredients were added. After another 2 min, carbon black was added. Compounding was carried out for 15 min at the same conditions. The mixing procedure for the blank sample (FKM) was the same as that of sample 10CB except no carbon black was added. The cure characteristics of the compounds were studied using a Moving Die Rheometer (MD+) operated at 160°C. The composites were denoted in the format XY, where the X denotes the concentration of the filler and Y the type of filler (i.e., 1020A is used for 10 phr of Cloisite 20A). Table I describes the formulation of the composites.

### Vulcanization, sample preparation, and testing

For X-ray diffraction (XRD) characterization, samples of 25 mm diameter, and 2 mm thickness were prepared by compression molding. Approximately, 2 g of sheeted out compounds were molded in a hydraulic-hot press, at 160°C and 10 MPa for a duration of five times the cure time ( $T_{c90}$ ) values. Since no reversion or marching was observed for the formulations, extension of curing time ensures that the compound reaches uniform crosslink density throughout the sample. The compression molded samples were conditioned for 1 day before testing. Samples for tensile, tear, and hardness tests were prepared using the same procedure explained above but using a mold cavity dimension of 150 mm × 150 mm × 2 mm. Dumbbell-shaped tensile samples and trouser-tie-shaped tear samples were punched out from the slabs prepared. For dynamic mechanical and thermal analysis (DMTA), the unused portion of tensile slabs were used and cut to the required dimension.

XRD was performed using a Rigaku diffractometer (CoK $\alpha$  = 0.1789 nm) operated at room temperature in the range of 2–10°. Tensile and tear tests were performed according to ASTM D412 and D624, respectively. Figure 1 shows the dimensions of the trouser-tie tear test sample along with the position

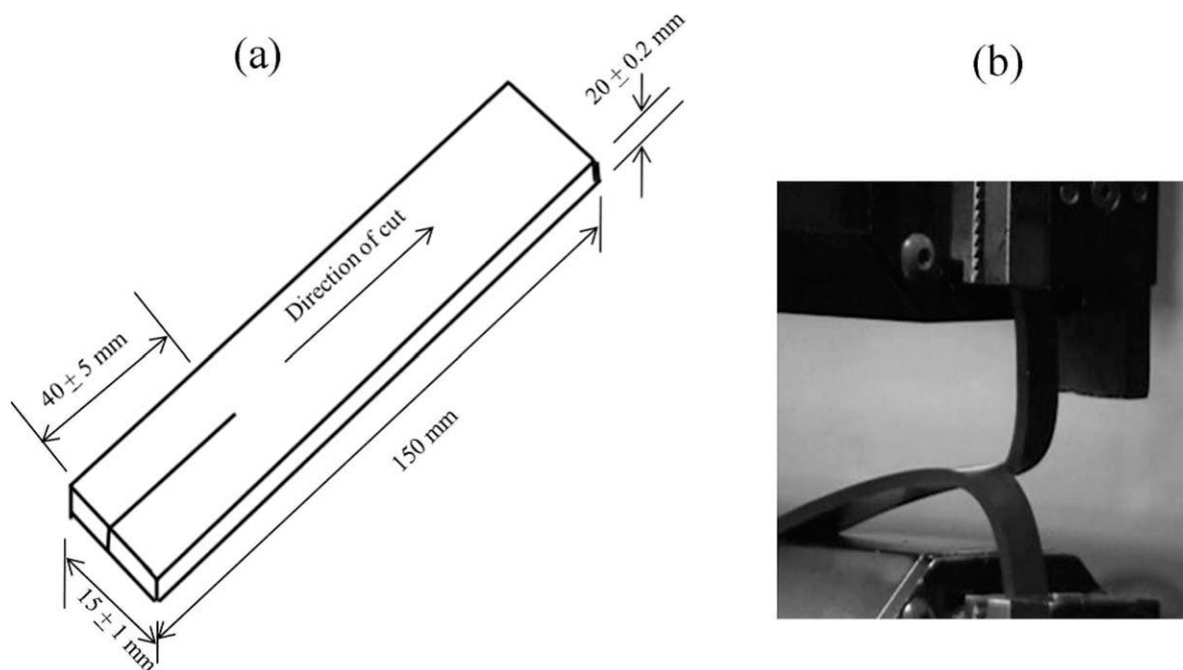


**Figure 1** (a) Dimensions of tear sample, (b) Tear sample clamped in testing machine (ASTM D624).

of the sample in a TensiTech testing machine. The test rate for tensile test was 500 mm/min and for tear strength was 50 mm/min. Shore A indentation hardness tester (ASTM D2240) was used to measure hardness. Strain-sweep experiments were performed in a Rheometrics DMTA V under three-point bending mode, at room temperature (30°C) and at a frequency of  $125 \text{ s}^{-1}$  between the strains 0 and 10%.

TEM analysis of the nanocomposites was carried out from ultra-cryomicrotomed sample sections on copper grids using a JEOL 2010 TEM at an accelerating voltage of 200 kV. Samples previously vulcanized were ultra-cryomicrotomed to sections of  $\sim 70$  nm in thickness using a Ultracryo-microtome Leica EM UC6.

## RESULTS AND DISCUSSION

### Morphology changes after vulcanization

In this section, the morphology of uncured FKM/clay composites is compared with the morphology of corresponding vulcanizates. As mentioned in the experimental section, after the preparation of the uncured rubber/clay composites, they were further compounded in the internal mixer and press-cured to obtain rubber/clay vulcanizates. Therefore, any changes in morphology had to have occurred during internal mixing and/or press-curing.

Figure 2 shows the X-ray diffractograms of the different organoclays and organoclay/FKM composites before and after vulcanization. It is worth mentioning that for unmodified clay (CloisiteNA), mixing

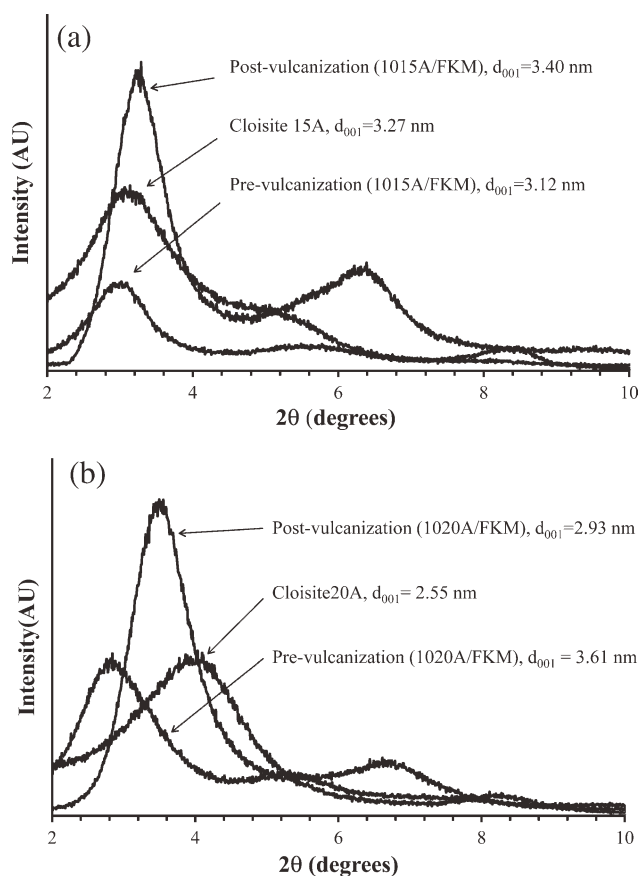


**Figure 2** Wide angle X-ray (WAX-D) diffractograms for organoclays and organoclay/FKM nanocomposites before and after vulcanization (a) 1015A/FKM composite (b) 1020A/FKM composite.

and vulcanization did not change the morphology of this composite and  $d$ -spacing of 1.21 nm was retained. However, in the composite filled with 10 phr Cloisite 15A (Fig. 2), the peak corresponding to the  $d_{001}$  reflection of the vulcanized sample shows a slight but definite shift to higher angles indicating that the clay  $d$ -spacing in the vulcanizate is lower than that in the masterbatch. The  $d$ -spacings of masterbatch and vulcanizate were 3.40 and 3.12 nm, respectively. It is not surprising that the  $d$ -spacing of the vulcanizate is lower than that of the clay 15A (3.27 nm) because the original  $d$ -spacing in 15A clay is high due to unbound surfactant in the galleries. However, the unbound surfactant is prone to being flushed out of the clay galleries as the authors have discussed earlier.<sup>12</sup> In Figure 2(b), a decrease of  $d$ -spacing is clearly seen for 10 phr Cloisite 20A/FKM evident from the shift of XRD peak to higher angle. The vulcanizate  $d$ -spacing is about 2.93 nm located between the  $d$ -spacings of pure Cloisite20A and masterbatch.

As mentioned above, either or both of the two processes, i.e., vulcanization and compounding can contribute to morphological changes in the vulcanizates. The internal mixing conditions during compounding do not differ greatly from those of the mixing process for preparing rubber/filler masterbatches. Therefore, compounding can be considered as an extension of the initial mixing process. However, the vulcanization process may have more of an effect on morphology, since it involves heating to a temperature of 160°C and exerting high pressure (10 MPa) for a significant amount of time. Moreover, vulcanization induced changes in morphology have been reported in previous studies.<sup>9–11</sup> This suggests that vulcanization plays a more important role in the observed morphological changes. For vulcanization-induced changes (e.g., deintercalation or restacking of clay layers), two reasons previously cited are the interference of organic intercalants in the curing reaction<sup>13–18</sup> and the effect of curing pressure.<sup>9–11</sup> As the organic amines in organoclays possess a similar chemical structure to that of accelerators used in sulfur-cures, when they are extracted out of the clay layers, they can participate in curing reactions, thereby causing the clay layers to collapse. In contrast, such reactions have not been reported for peroxide curing of elastomers. For these compounds, it was hypothesized that, at high molding pressure and high temperature, the clay platelets may restack in the elastomer matrix and then subsequently, there is a reduction in gallery spacing due to the pressure pushing platelets together.<sup>9</sup> More evidence for this pressure effect is given by the fact that in oven-cured composites without pressure, this deintercalation behavior is absent.<sup>9</sup> For the present case, the deintercalation in

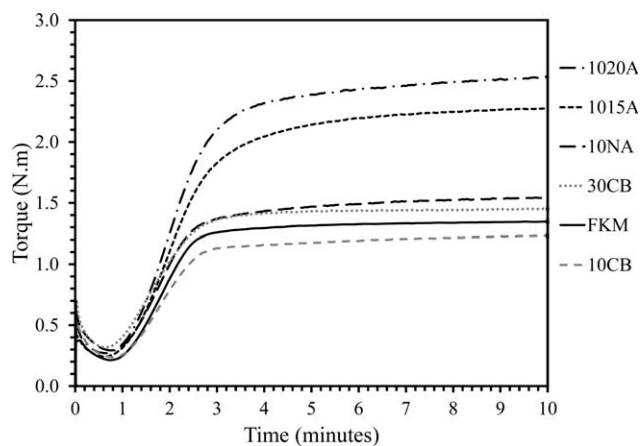


**Figure 3** Rheographs of different clay/FKM and carbon black/FKM composites.

1015A and 1020A is thought to be the result of high pressure curing during the compression molding process.

### Vulcanization characteristics

The vulcanization behavior of organoclay-filled composites has been a subject of intense discussion in earlier studies.<sup>6,7,19,20</sup> The discussion is mainly centered around the role of the organic surfactant present in modified clays and its ability to influence the crosslinking reaction rate and reaction extent. Figure 3 shows the rheographs of the clay-filled and carbon black-filled vulcanizates along with the gum (unfilled) vulcanizate. It is very obvious from the plot that organoclay filled compounds (1015A and 1020A) show a drastically different curing behavior than the rest of the compounds studied including the compound prepared with unfunctionalized clay (10NA).

When comparing the rheographs of different rubber compounds, a curve with higher storage modulus or higher maximum torque ( $M_H$ ) results from higher stiffness. Usually, such an increase in stiffness is attributed to either higher crosslinking density or reinforcement due to filler addition. It has been widely reported that the amines in nanoclays can influence sulfur curing resulting in increased crosslink density.<sup>5,21</sup> On the other hand, previous studies on peroxide curing of elastomer nanocomposites suggest that the nanoclay cannot influence the crosslink density of peroxide-cured vulcanizates.<sup>22,23</sup> Table II shows that significantly higher  $M_H$  were obtained for the composites prepared with organoclays (2.28 and 2.53 N/m for 15A and 20A, respectively) versus other composites (14.5 N/m for 30CB). Therefore, since a peroxide cure was used, the higher  $M_H$  observed in 1015A and 1020A (Fig. 3) is probably the result of reinforcement caused by

**TABLE II**  
Vulcanization Characteristics from Rheocurves for FKM, Carbon Black/FKM, and Clay/FKM Composites

Sample	$T_{s2}$ (min)	$T_{c90}$ (min)	CRI	$M_H$ (N/m)	$M_L$ (N/m)	$M_H - M_L$ (N/m)
FKM	1.4	2.8	71.4	1.36	0.21	1.15
10CB	1.5	3.2	58.8	1.24	0.24	1.00
30CB	1.3	2.8	66.7	1.45	0.32	1.13
10NA	1.4	3.7	43.5	1.54	0.29	1.25
1015A	1.3	4.2	34.5	2.28	0.24	2.04
1020A	1.3	3.9	38.5	2.53	0.27	2.26

$$\text{Cure rate index: CRI} = 100/(T_{c90} - T_{s2}).$$

organoclays. In our earlier study, the rheological behavior of uncured 15A and 20A filled composites indicated that these clays exhibited more significant reinforcement of FKM.<sup>12</sup> The reason that 1015A has lower  $M_H$  compared with 1020A can be attributed to its higher content of unbound intercalant, which will plasticize the compound when it is flushed out of the clay galleries. Unmodified clay-filled composite (10NA) shows a similar maximum torque value to that of the unfilled composite, because there is no significant reinforcement. The slight decrease of maximum torque in the case of 10 phr carbon black-filled composite is hard to explain as this behavior is usually not seen with most reinforcing fillers. Even a higher concentration of carbon black (30 phr) did not result in significant change in the rheocurve for FKM composite. The torque value, a function of both curing state and filler reinforcement, begins to sharply increase after 1 min in the case of nanocomposites (1015A and 1020A). As a result, the slope of the curing region of the rheograph is much higher for organoclay/FKM nanocomposites. This increase is caused by the increased stiffness due to clay dispersion combined with the effect of crosslinking.

Table II shows the scorch time and cure times of the composites. The scorch times ( $T_{s2}$ ) of all composites fall within a narrow range and show that the  $T_{s2}$  is not significantly affected by the presence of clay and organoclays. However, curing time ( $T_{c90}$ ), similar to  $M_H$ , was drastically affected by organoclays. From Table II, the authors can see that nanoclays tend to retard the vulcanization process (i.e.,

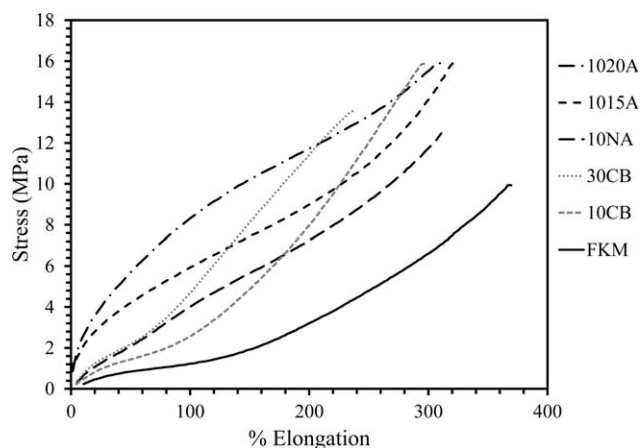


**Figure 4** Tensile test curves for FKM, clay/FKM and carbon-black/FKM composites.

they give higher  $T_{c90}$ ). The cure rate index was the lowest for the composite prepared with Cloisite15A, which indicates that the retardation effect is stronger in the presence of higher concentrations of intercalating surfactant in the composite. Such retardation with peroxide curing has been previously reported in published reports and it was suggested that it could be due to the scavenging of free radicals by organoclays.<sup>23</sup>

### Mechanical properties

Figure 4 and Table III show the tensile results for all composites and the crosslinked gum compound. The tensile properties of FKM improved upon adding 10 and 30 phr carbon black but improved more significantly upon adding organoclays. It is very clear that organoclays drastically change the stress-strain relationship, especially in the lower-strain region (<100%). 1015A and 1020A vulcanizates show increases of 400 and 583%, respectively, in 100% modulus compared with the blank compound (see Table III). The 10NA composites also show increases in 100% modulus but not as significant as in the case of nanocomposites prepared with organoclays.

When a rigid entity is dispersed in a liquid, it results in an increase in viscosity; whereas in an

**TABLE III**  
Tensile Test Results for FKM, Carbon Black/FKM, and Clay/FKM Composites

Sample	Tensile strength (MPa)	Elongation at break (%)	Modulus 100% (MPa)	Modulus 200% (MPa)	Hardness (Shore A)	Tear strength (kN/m)
FKM	9.49	354.04	1.2	3.29	60	22
10CB	16.04	301.51	2.5	7.78	67	27
30CB	13.15	241.76	4.4	10.89	75	26
10NA	12.89	315.94	4.0	7.32	70	40
1015A	16.12	322.04	6.0	9.08	80	46
1020A	15.98	311.87	8.2	11.72	85	67

elastomer, it imparts higher modulus to the matrix.<sup>24</sup> Such reinforcement arises from the hydrodynamic effect of the filler, which in turn is dictated by the shape factor (i.e., aspect ratio) of dispersed filler. Clay platelets, when dispersed, have a much higher shape factor than conventional fillers and this results in an even higher increase in stiffness.<sup>25</sup> This partially explains the large increase in modulus observed in 1015A and 1020A nanocomposites. The small fraction of polymer trapped in nanoclay galleries in the case of intercalated nanocomposites behaves like filler rather than polymer and thus leads to an increase in the effective volume fraction of filler in the matrix. This further contributes to the hydrodynamic reinforcement. The reason for 1015A exhibiting a lower modulus than 1020A can be ascribed to the same argument presented in the analysis of vulcanizates, i.e., higher amount of unbound surfactant in 1015A plasticizes the matrix. This highlights the importance of the concentration of surfactant in the organoclays.

In addition to the hydrodynamic effect, strong rubber–filler interaction is also needed to provide sufficient reinforcement to the matrix, particularly, when the strain increases. For an elastomer to have high fracture strength, it must be able to dissipate energy.<sup>26</sup> When a rubber composite is stretched, energy dissipation usually occurs due to hysteresis loss, which develops from the rubbing action of elastomer molecules on the filler surface. Therefore, hysteresis loss mainly depends on the adhesion between rubber and filler. When clays are intercalated by the polymer, more clay surface is in contact with the elastomer chains, which then increases the resistance to rubbing action, and thus increases hysteresis. This would increase the stress needed to bring about the same level of extension. This explains the improved modulus and tensile strength obtained for organoclay/FKM nanocomposites. Usually an increase in tensile strength properties results in substantial reduction in elongation; but this was not the case with organoclay/FKM nanocomposites. It was previously shown that higher elongation in the presence of filler can be due to irreversible orientation of elastomer chains at the filler surface, which reduces the retractive force but enhances the capability to extend in the direction of applied strain.<sup>27</sup> The retention of elongation properties is thought to be related to the higher surface area of nanoclay, since more filler surface area aids in the orientation of elastomer chains in the direction of strain. Although 10 phr carbon black provided only small enhancement in tensile modulus, it imparted similar tensile strength as that of nanoclay. This suggests that CB has an efficient energy release mechanism but poor hydrodynamic effect due to the roughly spherical shape of carbon black particles.

Table III shows the Shore A hardness and trouser-tie tear strength of the composites. The hardness, which is an indicator of level of reinforcement,<sup>21,25</sup> follows the same trend as that observed for the tensile modulus. Organoclays resulted in compounds with higher shore A hardness (80 and 85 for 10 phr of 15A and 20A, respectively). In addition, a significant increase in tear strength of the composites containing organoclays was observed (67 kN/m for 10 phr 20A versus 26 kN/m for 30 phr carbon black). This also correlates to other mechanical properties like hardness and modulus.

The analysis of the tear curves gives some understanding of the mechanism of elastomer reinforcement. Usually tear curves can be classified as having a smooth or knotty pattern. In this study, FKM, 10CB, and 10NA showed knotty tear patterns and 1015A and 1020A showed smooth tear patterns. During tearing of a carbon black-filled composite (10CB), as the crack-tip advances, the crack proceeds in the path offering least resistance, traveling from one filler particle to another and prolonging the tear significantly.<sup>28</sup> This type of crack advance results in a knotty tear pattern. Tear strength data shows that the nanocomposites prepared with organoclays exhibit significantly higher tear strengths than other composites studied. In conventional compounds, an enhancement in tear strength is usually accompanied by a presence of knotty tear pattern. However, smooth tearing gives higher tear strength in nanocomposites. De and Gent proposed that even with smooth tearing, significantly improved tear strength can be obtained, if the composites possess enhanced hysteresis.<sup>29</sup> It was mentioned earlier that intercalated nanocomposites can have higher hysteresis because the intercalated structure offers higher resistance to rubbing action between clay and filler due to the higher surface area. The difference in tear strength between 1015A and 1020A is quite significant. The reason why 1015A has lower tear strength value than 1020A is that a higher quantity of unbound surfactant in 1015A could lead to slip between elastomer and clay platelets, which would then drastically reduce the tear strength.

### Dynamic mechanical properties

The results of dynamic mechanical analysis (strain sweep) performed at room temperature are shown in Figure 5. The results indicate that 1020A and 1015A possess about four to five times the storage modulus of composites made with 10NA and 10CB at low strains. This reveals the advantage of the nanoreinforcement. It was discussed in earlier sections that the reinforcement arises from a combination of hydrodynamic effect and rubber–filler interaction. In carbon black-filled compounds, in addition

to these two factors, filler-networking also plays a major role.<sup>30</sup> However, the filler-networking effect has only been observed in the low-strain range and the network tends to break down at higher strains. DMTA analysis of nanocomposites performed under strain-sweep mode shows this behavior. It was reported that nanocomposites exhibit filler-networking in well intercalated (or exfoliated) compounds, and the filler-networking effects are greater, when the clay tactoids are expanded and the distance between tactoids reduces.<sup>25</sup> For the nanocomposites, the storage and loss modulus of 1015A and 1020A begin to decrease after a strain of about 1%. Above 1%, the filler networks break down. Composites made with 10 phr carbon black did not show any filler-networking. This may be due to the lower-surface area and the large-particle size of medium thermal black, which does not lead to a network at this filler concentration. However, at high strains, it can be seen that the slope of the storage and loss modulus of the composites tends to suddenly change at a certain strain value. This behavior was reported earlier with FKM composites and was attributed to the

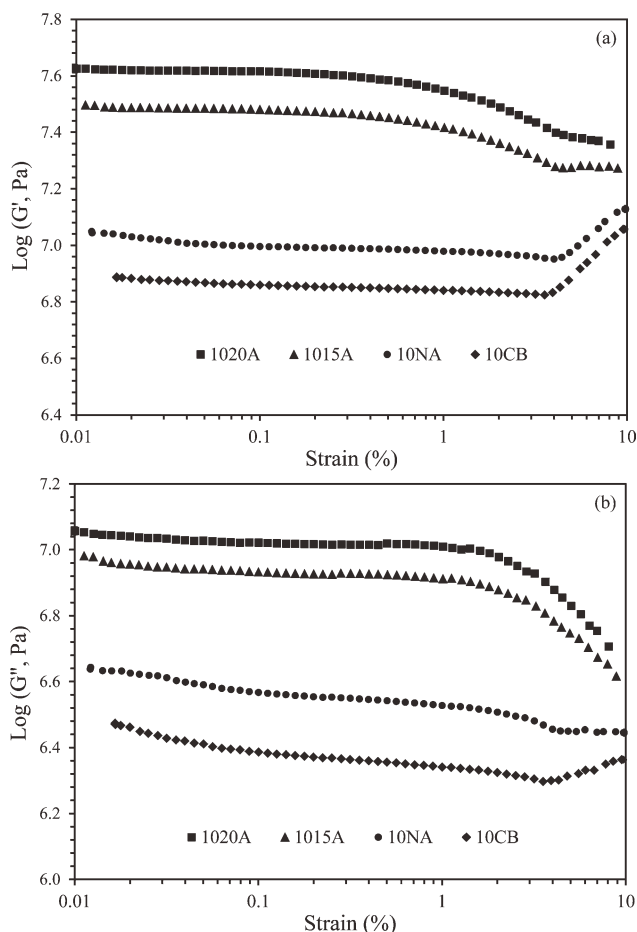
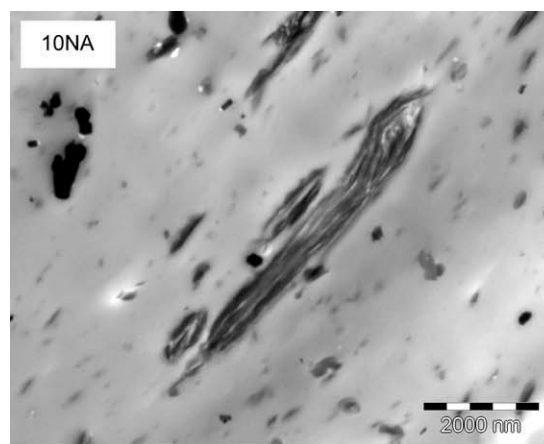
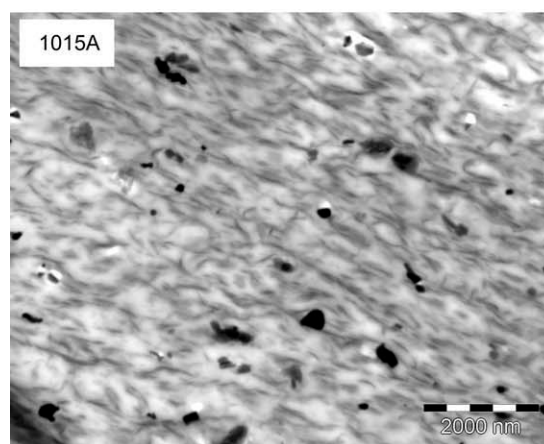


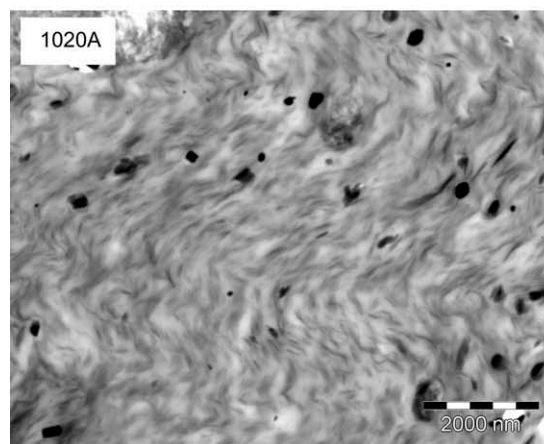
**Figure 5** Storage modulus (a) and loss modulus (b) as a function of the strain amplitude of clay/FKM and carbon-black/FKM composites.



(a)



(b)



(c)

**Figure 6** TEM images of clay/FKM nanocomposites.

crystallization of the VDF units in the FKM elastomer.<sup>31</sup>

### Morphological characterization

Figure 6 shows TEM micrographs of clay/FKM composites prepared with unmodified clay and organoclays. The morphology of the composites prepared with unmodified clay consists of large tactoids with

limited degree of dispersion at the nanolevel. In comparison, TEM images at same magnification of samples prepared with organoclays indicated significant dispersion of the organoclays at the nanoscale and suggested a mixture of intercalated and exfoliated morphology. There is a large amount of clay platelets dispersed in the sample and there is no any striking difference between the morphologies of composites prepared with Cloisite15A and 20A. The level of dispersion supported the mechanisms behind the level of reinforcement seen using organoclays versus using the unmodified clay.

### CONCLUSIONS

Vulcanized FKM/clay nanocomposites were prepared by melt-mixing, and mechanical and dynamic mechanical properties were studied. Although surfactants in Cloisite15A and 20A were advantageous in enhancing the interaction with elastomer matrix, the results from this study indicate that an excess of intercalated surfactant in the clay had an unfavorable effect on mechanical and dynamic mechanical properties. The gallery spacing of intercalated clay reduces during high-pressure curing. Silicate layers were found to be mobile at such high pressure and temperature favoring deintercalation. Clay intercalation and exfoliation provide high stiffness to the elastomer matrix. Although, the rate of vulcanization of the elastomer is reduced in the presence of organoclays, a significant increase in mechanical properties was still obtained with organoclay addition. Dynamic mechanical properties clearly showed the presence of filler-networking in composites prepared with organoclays. The intercalated/exfoliated structures obtained for organoclay/FKM nanocomposites can increase both hydrodynamic reinforcement and hysteresis loss, giving rise to a mechanically stronger compound.

The authors would like to acknowledge Mr. Oscar Salazar and Mr. Richard Li from Weatherford Canada Partnership in Edmonton, Alberta, Canada for availability of testing equipment for elastomer characterization.

### References

1. Sinha Ray, S.; Okamoto, M. *Prog Polym Sci (Oxford)* 2003, 28, 1539.
2. Alexandre, M.; Dubois, P. *Mater Sci Eng R Rep* 2000, 28, 1.
3. López-Manchado, M. A.; Herrero, B.; Arroyo, M. *Polym Int* 2004, 53, 1766.
4. Arroyo, M.; López-Manchado, M. A.; Herrero, B. *Polymer* 2003, 44, 2447.
5. Mousa, A.; Karger-Kocsis, J. *Macromol Mater Eng* 2001, 286, 260.
6. Choi, D.; Abdul Kader, M.; Cho, B. H.; Huh, Y. I.; Nah, C. *J Appl Polym Sci* 2005, 98, 1688.
7. Kim, W.; Kang, B. S.; Cho, S. G.; Ha, C. S.; Bae, J. W. *Compos Interfaces* 2007, 14, 409.
8. Kader, M. A.; Nah, C. *Polymer* 2004, 45, 2237.
9. Liang, Y. R.; Lu, Y. L.; Wu, Y. P.; Ma, Y.; Zhang, L. Q. *Macromol Rapid Commun* 2005, 26, 926.
10. Lu, Y. L.; Li, Z.; Mao, L. X.; Li, Y.; Wu, Y. P.; Liang, Y. R.; Zhang, L. Q. *J Appl Polym Sci* 2008, 110, 1034.
11. Maiti, M.; Bhowmick, A. K. *J Polym Sci B Polym Phys* 2006, 44, 162.
12. Lakshminarayanan, S.; Lin, B.; Gelves, G. A.; Sundararaj, U. *J Appl Polym Sci* 2009, 112, 3597.
13. Gatos, K. G.; Karger-Kocsis, J. *Polymer* 2005, 46, 3069.
14. Gatos, K. G.; Százdi, L.; Pukánszky, B.; Karger-Kocsis, J. *Macromol Rapid Commun* 2005, 26, 915.
15. LeBaron, P. C.; Pinnavaia, T. J. *Chem Mater* 2001, 13, 3760.
16. Usuki, A.; Tugigase, A.; Kato, M. *Polymer* 2002, 43, 2185.
17. Varghese, S.; Karger-Kocsis, J. *J Appl Polym Sci* 2004, 91, 813.
18. Hwang, W. G.; Wei, K. H.; Wu, C. M. *Polym Eng Sci* 2004, 44, 2117.
19. López-Manchado, M. A.; Arroyo, M.; Herrero, B.; Biagiotti, J. *J Appl Polym Sci* 2003, 89, 1.
20. Avalos, F.; Ortiz, J. C.; Zitzumbo, R.; López-Manchado, M. A.; Verdejo, R.; Arroyo, M. *Eur Polym J* 2008, 44, 3108.
21. Karger-Kocsis, J.; Wu, C. M. *Polym Eng Sci* 2004, 44, 1083.
22. Zheng, H.; Zhang, Y.; Peng, Z. *Polym Polym Compos* 2004, 12, 197.
23. Mishra, J. K.; Kim, I.; Ha, C. S. *Macromol Rapid Commun* 2003, 24, 671.
24. Donnet, J. B. *Rubber Chem Technol* 1998, 71, 323.
25. Vu, Y. T.; Mark, J. E.; Pham, L. H.; Engelhardt, M. *J Appl Polym Sci* 2001, 82, 1391.
26. Hamed, G. R. *Rubber Chem Technol* 2000, 73, 524.
27. Edwards, D. C. *J Mater Sci* 1990, 25, 4175.
28. Rigbi, Z. *Rubber Chem Technol* 1982, 55, 1180.
29. De, D.; Gent, A. N. *Rubber Chem Technol* 1996, 69, 834.
30. Payne, A. R. *J Appl Polym Sci* 1962, 6, 57.
31. Maiti, M.; Bhowmick, A. K. *Polym Eng Sci* 2007, 47, 1777.